Venture into Water's No Man's Land: Structural Transformations of Solid H_{2}O under Rapid Compression and Decompression

Chuanlong Lin, Jesse S. Smith, Xuqiang Liu, John S. Tse, and Wenge Yang

Phys. Rev. Lett. **121**, 225703 — Published 30 November 2018

DOI: 10.1103/PhysRevLett.121.225703

Venture into water's no man's land: Structural transformations of solid H_2O under rapid compression and decompression

Chuanlong Lin[1], Jesse S. Smith[2], Xuqiang Liu[1,3], John S. Tse[1,4,*], Wenge Yang[1,*]

[1]Center for High Pressure Science and Technology Advanced Research, Shanghai 201203, China

[2] HPCAT, Geophysical Laboratory, Carnegie Institution of Washington, Argonne, Illinois 60439, USA

[3] Key Laboratory for Anisotropy and Texture of Materials, School of Material Science and Engineering, Northeastern University, Shenyang 110819, China

[4] Department of Physics and Engineering Physics, University of Saskatchewan, Saskatoon, S7N 5E2 Canada

∗Correspondence: yangwg@hpstar.ac.cn and john.tse@usask.ca

Abstract: Pressure-induced formation of amorphous ices and low-density amorphous (LDA) to high-density amorphous (HDA) transition have been believed to occur kinetically below a crossover temperature (T_c) above which thermodynamically-driven crystalline-crystalline (*e.g.*, ice Ih-to-II) transitions and crystallization of HDA and LDA are dominant. Here we show compression-rate dependent formation of a high-density non-crystalline (HDN) phase transformed from ice Ic above T_c, bypassing crystalline-crystalline transitions under rapid compression. Rapid decompression above T_c transforms HDN to a low-density non-crystalline (LDN) phase which crystallizes spontaneously into ice Ic, whereas slow decompression of HDN leads to direct crystallization. The results indicate the formation of HDA and the HDN-to-LDN transition above T_c are results of competition between (de)compression rate, energy barrier and temperature. The crossover temperature is shown to have an exponential relationship with the threshold compression rate. The present results provide important insight into the dynamic property of the phase transitions in addition to the static study.

Pressure-induced amorphization of ice Ih and the transformation between low-density amorphous (LDA), high-density amorphous (HDA) and very high-density amorphous (VHDA) ices are of fundamental importance in the study of the physics and chemistry of ice, and have become the prototypical examples in the investigation of amorphization and amorphous-amorphous transitions for many materials [1-6]. The first-order-like LDA-to-HDA transition--extrapolated into so-called water's no man's land where the temperature is between homogeneous nucleation temperature (T_H) [7, 8] of supercooled water and crystallization temperature (T_X) [9-12] of amorphous ice, has been hypothesized to terminate at a second critical point (~110 Mbar and ~220 K) [13] and, was considered as indication of a low-density liquid (LDL) to high-density liquid (HDL) transition [14-17]. Both phenomenon, pressure-induced amorphization of ice Ih and the LDA-to-HDA transition, were cornerstones of the two-liquid model of water [14-16]. However, studies on the transition mechanism, atomic structures of the non-crystalline phases (namely, LDA, HDA, VHDA, LDL and HDL) and polyamorphous transition have been hindered by the thermodynamically-driven crystalline-crystalline transition and rapid crystallization at higher temperatures [10-12, 18-20], leaving a large temperature range (~140-220 K) unexplored.

In 1990's, a study of emulsified-confined ice Ih indicated a crossover temperature (T_c) at ~160 K at which the phase transition mechanism changes from a thermodynamically-driven transition to mechanical instability [17, 21], suggested by quasi-harmonic lattice-dynamics calculations [22, 23]. Recently, *in-situ* synchrotron x-ray diffraction measurements on bulk water have shown that the crossover temperature occurs at ~145 K [20]. Ice Ih was found to undergo kinetically-controlled amorphization under slow compression (<0.01 GPa/s) of ice Ih up to 1.2 GPa below 145 K. Above 145 K, a thermodynamically-driven crystalline-crystalline transition from ice Ih to crystalline ice II (or IX) occurs instead of amorphization. So far, exploration on amorphization of ice Ih and LDA-to-HDA transition is limited up to ~140 K due to rapid crystallization of amorphous ices at higher temperatures [9, 20, 24], even though LDA and HDA have been studied extensively for the glass-liquid transition and LDL-to-HDL transition below T_X [10-12, 18, 19, 25, 26].

Previous studies have shown that it is possible to bypass crystalline-crystalline transitions and form non-crystalline phases by rapid/shock (de)compression [27-30]. For instance, amorphous silicon can be obtained from high-pressure crystalline phase by rapid (or shock) (de)compression [27, 29]. For ice, the phase transitions have been found to be (de)compression-rate dependent. Bauer *et al.* found that ice Ih transformed to ice II under slow compression and to ice III at a moderately higher compression rate (~4 GPa/min) at 170 K [31]. Chen *et al.* reported a high-density amorphous ice by rapid compression of liquid water at room temperature [32]. Recently, the high-pressure ice VIII was reported to undergo a metastable melting into a deeply supercooled low-density non-crysstalline phase under rapid decompression at temperatures of 140-165 K [33]. Motivated by these earlier works, here we examine the possible formation of a high-density non-crystalline (HDN) phase from ice Ic and LDA-to-HDA transition above T_c, bypassing the thermodynamically-driven crystalline-crystalline transitions and crystallization of the non-crystalline phases under rapid (de)compression using fast *in-situ* x-ray diffraction measurement [29, 34]. We show that ice Ic transforms to a high-density non-crystalline phase above T_c under rapid compression. Moreover, under rapid decompression above T_c, the crystallization process can be suppressed and a polyamorphous transition is observed in HDN. Here, the transformed amorphous ice phase above T_c (*i.e.* within the no man's land) is labelled as HDN to distinguish it from the HDA phase obtained from the pressurization of ice Ih below 145 K [20]. The purpose is to emphasize that the crystalline → amorphous transition can occur in this temperature-pressure region. We do not assert it is a different kind of amorphous state.

The experimental details have been described in previous studies [20, 33] and can be found in the supplementary material [35]. In the present work, ice Ic was used as the starting material. It was prepared by decompressing high-pressure ice VIII from 4 GPa (or >4 GPa) to ~1 Pa at 180 K, during which the sample ice underwent VIII→ VI→ II→ Ic transitions. Then the ice Ic phase was cooled from 180 K to a given temperature in preparation for rapid/slow compression. Figure 1(a) and (b) show the comparison of experimental results under slow/rapid compression at 164 K. Under slow compression at 164 K, ice Ic transforms to ice II at ~0.2 GPa, then to ice VI at ~ 1.7 GPa and finally to ice VIII at 3.9 GPa [Fig. 1(a)]. At moderately higher compression rate, ice Ic transforms

to ice IX phase, followed by ice IX→ ice VI→ ice VIII transitions (Fig. S1). This is consistent with previous reports on the compression-rate dependent crystalline-crystalline transitions at 170 K [31]. However, under rapid compression (~14.8 GPa/s) from ~1 Pa to 3.5 GPa at 164 K, we found that ice Ic transforms to a non-crystalline phase at ~1.3 GPa with a broad diffraction peak at Q=2.27 Å^{-1}. The diffraction pattern of the non-crystalline phase shows the first broad peak shifted to a higher Q value of 2.40 Å^{-1} at ~2.8 GPa. Then it transforms to ice VIII at ~3.2 GPa under further compression [Fig. 1(b)]. Incidentally, the Q value of the non-crystalline phase is close to that of HDA at 1.3 GPa and to VHDA at ~2.8 GPa [20]. The observations indicate a high-density non-crystalline (HDN) phase is formed at 1.3 GPa, which subsequently transforms to a very high-density non-crystalline phase under further compression. This is similar to the occurrence of HDA and VHDA ices. Compared with the gradual crystallization of the very HDN phase, the formation of HDN is abrupt within a narrow pressure range [Fig. 1(b) and see integrated diffraction patterns in Fig.S2]. It should be noted that the starting sample used here is ice Ic. Structurally it is slightly different from ice Ih and the amorphization pressure is 0.05 GPa lower than ice Ih [40]. The present work does not suggest that ice Ih has the same compression-rate dependent amorphization above T_c, although the difference is expected to be small.

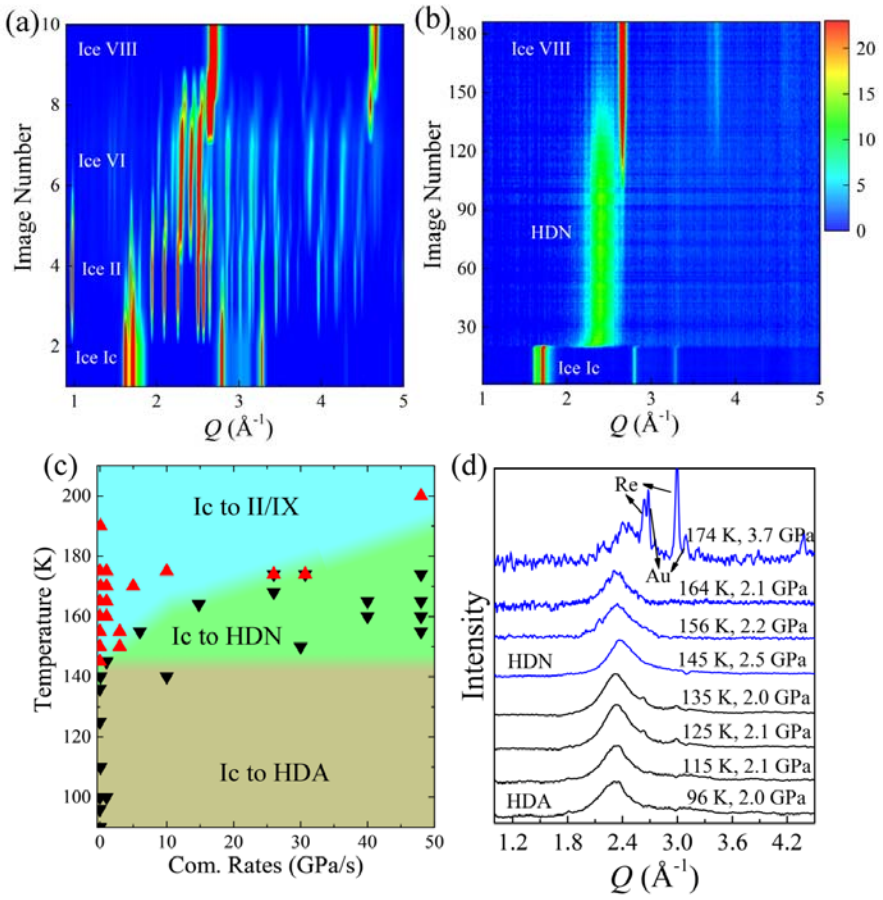

Fig. 1 Compression-rate dependent formation of high-density non-crystalline phase. (a) Under slow compression (<0.01 GPa/s) from ~1 Pa to 5 GPa at an interval of ~0.05 GPa with the pressure monitored by an on-line ruby system, the phase transition sequence of ice Ic → ice II → ice VI → ice VIII is observed. The diffraction data is acquired with exposure time of 5 s. (b) Under rapid compression from ~1 Pa to 3.5 GPa with a rate of ~14.8 GPa/s, ice Ic transforms to a non-crystalline phase first, followed by crystallization into ice VIII. During rapid compression, the pressure is increased continuously with the continuous collection of x-ray diffraction images. It should be noted that the rate changes during compression process. The rate of ~14.8 GPa/s is estimated in the pressure range where ice Ic to HDN transition occurs. The exposure time for each diffraction image is 50 ms with images collected at a frequency of 20 Hz. (c) Summary of compression-rate dependent phase transformation from ice Ic to high-density non-crystalline phase at different temperatures. (d) Comparison of the diffraction patterns of the non-crystalline phases at different temperatures. The high-density non-crystalline phases above 145 K are obtained from ice Ic under rapid compression. The HDA phases below 145 K are obtained by static compression of ice Ih [20].

In order to probe the effects of temperature and compression rate on the phase transitions, we have conducted systematic investigations at different temperatures and compression rates. Figure 1(c) summarizes the experimental results. It shows that the formation of HDN from ice Ic under rapid compression is also observed at a temperature range between 145 K and 174 K [Fig. 1(c) and Figs. S3 to S7], all above the previously reported crossover temperature (T_c ~145 K) [20]. At these temperatures and a moderate compression rate, however, ice Ic transforms to ice II or IX [Fig. 1(c)], followed by transformations to ice VI and VIII [20]. Above 145 K, the phase transformation of ice Ic is compression-rate dependent. This is in contrast to the compression-rate independent amorphization below 145 K. At a given temperature (T), it appears that there exists a threshold compression rate required for the formation of the HDN phase. Below 160 K, the minimum compression rate gradually increases as temperature increases. At T > 160 K, the compression rate required for producing the HDN phase increases rapidly with increasing temperature. Figure 1(d) shows the integrated diffraction patterns of HDN at different temperatures with background subtracted, compared with those of HDA transformed from ice Ih below 145 K. It is clearly seen that the diffraction patterns of the HDN phase are similar to those of HDA. From x-ray diffraction patterns, we cannot distinguish whether HDN is a solid amorphous ice or a viscous HDL as suggested previously [18, 26, 41-43], even though HDN is observed above the glass transition temperature of HDA.

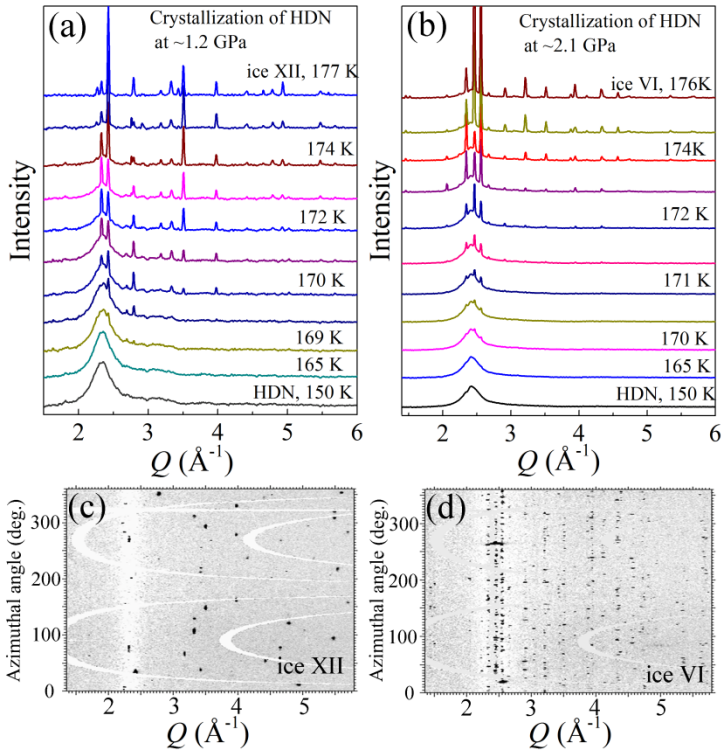

Fig. 2 Crystallization of high-density non-crystalline phase at 1.2 GPa and 2.1 GPa by warming. (a) HDN is heated from 150 K to 177 K. It starts to crystallize into ice XII at ~169 K, and completes at ~177 K. (b) HDN is heated from 150 K. It crystallizes into ice VI at ~170 K and is complete at ~176 K. (c) and (d) Azimuthally unwrapped x-ray diffraction images of ice XII and VI crystallized from HDN at ~1.2 GPa and ~2.1 GPa, respectively. The diffraction images, subtracted by an image of the non-crystalline phase as background, are obtained by caking (unrolling) the two dimensional x-ray diffraction images. The horizontal axis is Q value. The vertical axis is azimuth angle. The white broad band at ~2.3 $Å^{-1}$ indicates the first sharp peak of HDN. The black dots are the diffraction peaks from crystalline phases of ice XII and VI. The half-ellipses are the masks from the area detector.

The HDN sample at a given pressure is heated to monitor the stability and crystallization behavior. In the experiments, the HDN phase is obtained by rapid compression of ice Ic up to ~2.0 GPa at 150 K, and then the pressure is adjusted to the targeted value using double membrane pressure control [34]. Depending on the pressure, crystallization of the non-crystalline phase into different dense crystalline ices is observed (Figs. 2). It is found that the non-crystalline phase transforms to ice XII at ~1.2

GPa during heating from 169 K to 177 K [Fig.2(a)] and to ice VI at 2.1 GPa from 170 K to 176 K [Fig.2(b)]. The crystallization into different crystalline ices indicates that the non-crystalline phases at ~1.2 GPa and ~2.1 GPa may have different local structures, corresponding to HDA and VHDA. These observations are consistent with previous reports on *ex-situ* x-ray diffraction measurements [44]. Instead of the initial homogenous powder patterns, the diffraction patterns of ice XII and VI consist of sharp diffraction spots, indicating single crystals or polycrystalline grains of ice XII [Fig. 2(c)] and VI [Fig. 2(d)]. The results indicate grain coalescence during the crystallization process of the HDN phase. In contrast, there is no grain growth or grain coalescence in the crystalline-crystalline transitions (ice Ic→ ice II→ ice VI→ ice VIII) during compression.

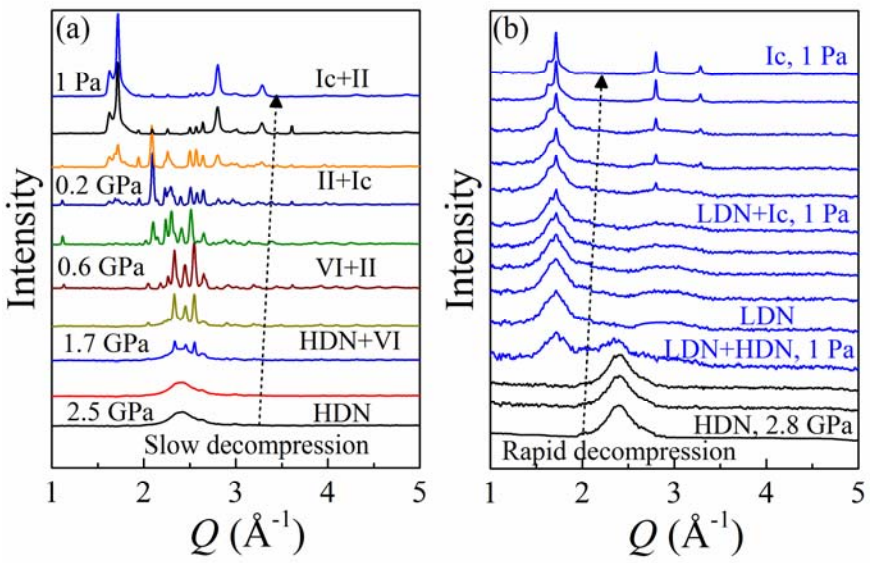

Fig. 3 Rate-dependent phase transformation of HDN at 158 K under decompression. (a) Slow decompression of HDN leads to crystallization into ice VI, followed by ice VI →ice II →ice Ic transitions. (b) Rapid decompression (~10 GPa/s) of HDN results in the direct transformation to a low-density non-crystalline phase.

Figure 3 shows the phase transitions of HDN under decompression at different ramp rates. In the experiments, HDN is obtained by rapid compression of ice Ic at 158 K. After observing the HDN phase, the pressure is released immediately at different decompression rates. We find the phase transition of HDN under decompression is dependent on the ramp rates. At a slow decompression rate (<0.01 GPa/s), HDN phase crystallizes into ice VI and transforms to ice II and eventually to Ic [Fig. 3(a)]. At a high

decompression rate (~10 GPa/s), instead of direct crystallization, the HDN phase is found to transform to a low-density non-crystalline phase (LDN) at ~1 Pa [Fig. 3(b)]. The LDN subsequently crystallizes into ice Ic. Previous results show that the LDN phase could be a deeply supercooled low-density liquid phase [33], indicated by the temperature-dependent crystallization behavior.

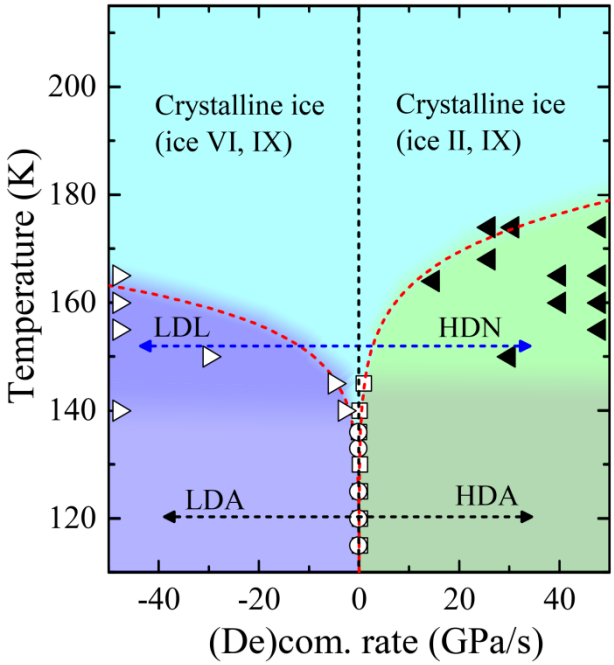

Fig. 4 (De)compression-rate (negative decompression, positive compression) dependent formation of non-crystalline phases at different temperatures. Black solid triangles represent high-density non-crystalline phase obtained by rapid compression in present work. Open squares and circles indicate the high-density amorphous and low-density phases previously obtained by static compression/decompression [20]. Open triangles are low-density non-crystalline phase formed from high-pressure ice VIII under rapid decompression [33]. Red dashing line is the fitting line.

Fig. 4 summarizes the compression-rate dependent formation of high-density non-crystalline phases at various temperatures, compared to the formation of low-density non-crystalline (LDA and LDL) phases. With increasing temperature, the minimum compression/decompression rate required for the formation of non-crystalline phases increases (Fig. 4). The threshold (de)compression rate has a steep initial increase at low temperature and slight increase at higher temperature. It should be noted that the

temperature at the threshold compression rate corresponds to a crossover temperature, namely, above which thermodynamically-driven crystalline-crystalline transitions (*i.e.*, ice Ic-to-II for compression and VIII-to-VI for decompression) are observed and below which the non-crystalline phases form. Noticeably, the transition temperature changes with compression rate. Therefore, how the threshold compression rate is related to the transition temperature (T_c)?

In order to bypass thermodynamically-driven Ic-to-II (or ice IX) transition at given temperature, the compression time (Δt), required for passing the equilibrium stable pressure range (ΔP) of ice II, should be shorter than the characteristic transition time (τ) of ice Ic-to-II transition. The transition time (τ) is determined by the Arrhenius equation [45-48], namely, $1/\tau \sim$ the rate constant which is proportional to $\mathrm{Exp}(-\Delta E/k_B T)$, where ΔE is the energy barrier for the phase transition and k_B is Boltzmann constant. The thermal energy ($k_B T$) governs the probability of the water to overcome the energy barrier. The compression time in bypassing the pressure region of ice II is determined by $\Delta t = \Delta P/\beta$, where β is the compression rate. The HDN phase is formed when $\Delta t < \tau$, namely, ice Ic bypasses the equilibrium pressure region of ice II on a shorter time scale so that ice Ic-to-II transition does not have enough time to occur. For simplicity, let us assume ΔE and ΔP are independent of pressure and temperature, the threshold compression rate (β_c) is determined by $\Delta t=\tau$. Then we can obtain $\beta_c=C_0*\exp(-\Delta E/k_B T_c)$, where C_0 is a constant with units of GPa/s. It is clear that the formation of the HDN phase is the result of competition among the external compression rate, temperature, and energy barrier. It is more complicated in reality as both ΔE and ΔP also change with pressure and temperature.

The red dash lines in Fig. 4 are fits of the experimental compression and decompression results to the Arrhenius law. Reasonable agreements are obtained with ΔE of 24(2) kJ/mol and C_0 of 6.4×10^8 GPa/s for compression and ΔE of 26(2) kJ/mol and C_0 of 1.3×10^{10} GPa/s for decompression. It should be noted that ΔE represents an average order of magnitude estimated as the value is expected to vary with pressure during (de)compression [48]. The characteristic time of ice Ic-to-II transition as a function of temperature can be estimated based on the fitting results. For example, τ is estimated to

be ~10^7 s for the formation of HDA at liquid nitrogen temperature, which is much longer than the experimental time scale (minutes or hours). This explains previous observations that ice Ih can bypass the pressure region of ice II and transforms to a metastable amorphous phase under compression to 1.2 GPa [20]. The previously reported HDA phase can be viewed as the case of slow compression (solid and open triangles in Fig. 4). With increasing temperature, τ decreases exponentially from ~10^7 s at 77 K to ~10^{-2} s at 174 K. Therefore, at high temperature, the characteristic time of the phase transition from 145K to 174 K is comparable to the experimental time scale. This interpretation is consistent with the observed compression-rate dependent phase transition pathway. Extrapolation of the present results to higher temperature towards the proposed second critical point (110 MPa, 220 K) [13] suggests the time scale is in the nano- to microsecond regime. The formation of HDN may still be possible but will require ultrafast *in-situ* measurement at a very high compression rate.

The mechanism of the decompression-induced HDA-to-LDA transition is also determined by the competition between the energy barrier for crystallization of the non-crystalline phases, temperature and decompression rate. Suppression of crystallization of HDN is observed in rapid decompression as the transformation from HDN to LDL can be observed above 140 K (blue arrow in Fig. 4). The present results expand the temperature range from the previous report on HDA-to-LDA transition (black arrow in Fig. 4). The well-known HDA-to-LDA transition below 140 K can be viewed as a case of slow decompression, analogous to the pressure-induced amorphization. At a given temperature, the threshold decompression rate for the formation of LDL from ice VIII [33] is larger than the minimum compression rate for formation of HDN from ice Ic. From the boundary between crystalline ice and non-crystalline phases shown in Fig. 4, the temperature range for the formation of LDL is apparently smaller than that of HDN, and there may be a critical temperature above which the transformation between HDN and LDL will not occur even with very rapid decompression.

The experimental evidences provided here clearly show the importance of role of kinetics in the structural phase transitions between crystalline and amorphous ices in the no man's land. The results show the suggestion of the existence of a critical temperature

Tc, the cross-over temperature between homogeneous nucleation and amorphization, is not founded on firm thermodynamic grounds. It is also shown this "imaginary" phase boundary can be traversed by rapid compression (*i.e.* controlling of the kinetics). The compression of ice Ih to HDA at low temperature is due to insufficient external energy to overcome the energy barrier required to rearrange the hydrogen bonds to the thermodynamically stable crystalline structure, possibly ice VI (or XV). We speculate that a crystalline → crystalline transition for ice Ih could eventually be achieved if compressed in a hydrostatic medium at a very slow rate allowing the relaxation of the frustrated intermediate amorphous structure. Moreover, the experimental decompression results show the HDN → LDN phase boundary does not extrapolate to the proposed second critical point.

Acknowledgements. The authors thank Curtis Kenney-Benson and Richard Ferry for technical support and like to thank the financial support from Science Challenge Project (TZ2016001) and National Nature Science Foundation of China (U1530402). HPCAT operations are supported by DOE−NNSA under Award DE-NA0001974, with partial instrumentation funding by NSF. APS is supported by DOE−BES, under Contract DE-AC02-06CH11357 by UChicago Argonne, LLC.

References

[1] O. Mishima, L. D. Calvert, and E. Whalley, Nature (London) 310, 393 (1984).
[2] O. Mishima, L. D. Calvert, and E. Whalley, Nature (London) 314, 76 (1985).
[3] R. J. Hemley, A. P. Jephcoat, H. K. Mao, L. C. Ming, and M. H. Manghnani, Nature (London) 334, 52 (1988).
[4] J. P. Itie, A. Polian, G. Calas, J. Petiau, A. Fontaine, and H. Tolentino, Phys. Rev. Lett. 63, 398 (1989).
[5] M. B. Kruger, and R. Jeanloz, Science 249, 647 (1990).
[6] L. Thomas, and G. Nicolas, J. Phys. Condens. Matter 18, R919 (2006).
[7] B. J. Mason, Adv. Phys. 7, 221 (1958).
[8] J. A. Sellberg, C. Huang, T. A. McQueen, N. D. Loh, H. Laksmono, D. Schlesinger, R. G. Sierra, D. Nordlund, C. Y. Hampton, D. Starodub, D. P. DePonte, M. Beye, C. Chen, A. V. Martin, A. Barty, K. T. Wikfeldt, T. M. Weiss, C. Caronna, J.

Feldkamp, L. B. Skinner, M. M. Seibert, M. Messerschmidt, G. J. Williams, S. Boutet, L.G.M. Pettersson, M. J. Bogan, and A. Nilsson, Nature (London) 510, 381 (2014).

[9] O. Mishima, J. Chem. Phys. 100, 5910 (1994).

[10] G.P. Johari, A. Hallbrucker, and E. Mayer, Nature (London) 330, 552 (1987).

[11] R. S. Smith, B. D. Kay, Nature (London) 398, 788 (1999).

[12] O. Andersson, Proc. Natl. Acad. Sci. U. S. A. 108, 11013 (2011).

[13] O. Mishima, and H. E. Stanley, Nature (London) 392, 164 (1998).

[14] P. H. Poole, F. Sciortino, U. Essmann, and H. E. Stanley, Nature (London) 360, 324 (1992).

[15] K. Amann-Winkel, R. Bohmer, F. Fujara, C. Gainaru, B. Geil, and T. Loerting, Rev. Mod. Phys. 88, 011002 (2016).

[16] P. Gallo, K. Arnann-Winkel, C. A. Angell, M. A. Anisimov, F. Caupin, C. Chakravarty, E. Lascaris, T. Loerting, A. Z. Panagiotopoulos, J. Russo, J. A. Sellberg, H. E. Stanley, H. Tanaka, C. Vega, L. M. Xu, and L. G. M. Pettersson, Chem. Rev. 116, 7463 (2016).

[17] O. Mishima, and H. E. Stanley, Nature (London) 396, 329-335 (1998).

[18] C. Hill, C. Mitterdorfer, T. G. A. Youngs, D. T. Bowron, H. J. Fraser, and T. Loerting, Phys. Rev. Lett. 116, 215501 (2016).

[19] F. Perakis, K. Amann-Winkel, F. Lehmkühler, M. Sprung, D. Mariedahl, J. A. Sellberg, H. Pathak, A. Späh, F. Cavalca, D. Schlesinger, A. Ricci, A. Jain, B. Massani, F. Aubree, C. J. Benmore, T. Loerting, G. Grübel, L. G. M. Pettersson, and A. Nilsson, Proc. Natl. Acad. Sci. U. S. A. 114, 8193 (2017).

[20] C. L. Lin, X. Yong, J. S. Tse, J. S. Smith, S. V. Sinogeikin, C. Kenney-Benson, and G. Y. Shen, Phys. Rev. Lett. 119, 135701 (2017).

[21] O. Mishima, Nature (London) 384, 546 (1996).

[22] J. S. Tse, D. D. Klug, C. A. Tulk, I. Swainson, E. C. Svensson, C. K. Loong, V. Shpakov, V. R. Belosludov, R. V. Belosludov, and Y. Kawazoe, Nature (London) 400, 647 (1999).

[23] J. S. Tse, J. Chem. Phys. 96, 5482 (1992).

[24] E. L. Gromitskaya, O. V. Stal'gorova, V. V. Brazhkin, and A. G. Lyapin, Phys. Rev. B 64, 094205 (2001).

[25] M. S. Elsaesser, K. Winkel, E. Mayer, and T. Loerting, Phys. Chem. Chem. Phys. 12, 708 (2010).

[26] K. Amann-Winkel, C. Gainaru, P. H. Handle, M. Seidl, H. Nelson, R. Böhmer, and T. Loerting, Proc. Natl. Acad. Sci. U. S. A. 110, 17720 (2013).

[27] M. Gamero-Castano, A. Torrents, L. Valdevit, and J. G. Zheng, Phys. Rev. Lett. 105, 145701 (2010).
[28] S. T. Zhao, B. Kad, C. E. Wehrenberg, B. A. Remington, E. N. Hahn, K. L. More, and M. A. Meyers, Proc. Natl. Acad. Sci. U. S. A. 114, 9791 (2017).
[29] J. S. Smith, S. V. Sinogeikin, C. L. Lin, E. Rod, L. G. Bai, and G. Y. Shen, Rev. Sci. Instrum. 86, 072208 (2015).
[30] D. R. Clarke, M. C. Kroll, P. D. Kirchner, R. F. Cook, and B. J. Hockey, Phys. Rev. Lett. 60 2156 (1988).
[31] M. Bauer, M. S. Elsaesser, K. Winkel, E. Mayer, and T. Loerting, Phys. Rev. B 77, 220105 (2008).
[32] J. Y. Chen, and C. S. Yoo, Proc. Natl. Acad. Sci. U. S. A. 108, 7685 (2011).
[33] C. Lin, S. S. Smith, S. V. Sinogeikin, and G. Shen, Proc. Natl. Acad. Sci. U. S. A. 115, 2010-2015(2018).
[34] S. V. Sinogeikin, J. S. Smith, E. Rod, C. L. Lin, C. Kenney-Benson, and G.Y. Shen, Rev. Sci. Instrum. 86, 072209 (2015).
[35] See Supplemental Material at [url] for experimental detials, which includes Ref. [36-39].
[36] R. Hrubiak, S. Sinogeikin, E. Rod, and G. Y. Shen, Rev. Sci. Instrum., 86, 072202 (2015).
[37] H. K. Mao, J. Xu, P. M. Bell, J. Geophys. Res. 91, 4673-4676 (1986).
[38] J. Yen, M. Nicol, J. Appl. Phys. 72, 5535-5538 (1992).
[39] C. Prescher, V.B. Prakapenka, High Press. Res. 35, 223-230 (2015).
[40] M. A. Floriano, Y. P. Handa, D. D. Klug, and Edward Whalley, J. Chem. Phys. 91 7187-7192 (1989).
[41] T. Loerting, V. Fuentes-Landete, P. H. Handle, M. Seidl, K. Amann-Winkel, C. Gainaru, and R. Bohmer, J. Non-Cryst. Solids, 407, 423 (2015).
[42] P. H. Handle, M. Seidl, and T. Loerting, Phys. Rev. Lett. 108, 225901 (2012).
[43] M. Seidl, M.S. Elsaesser, K. Winkel, G. Zifferer, E. Mayer, and T. Loerting, Phys. Rev. B 83, 100201(2011).
[44] S. Klotz, G. Hamel, J. S. Loveday, R. J. Nelmes, and M. Guthrie, Z. Kristallogr. 218, 117 (2003).
[45] N. V. C. Shekar, and K. G. Rajan, Bull. Mater. Sci. 24, 1 (2001).
[46] A. K. Singh, Mater. Sci. Forum, 3, 291 (1985).
[47] S. Glasstone, K. J. Laidler, H. Eyring, The Theory of Rate Processes (McGraw-Hill, New York, 1941).

[48] C. L. Lin, J. S. Smith, S. V. Sinogeikin, C. Park, Y. Kono, C. Kenney-Benson, E. Rod, and G. Y. Shen, J. Appl. Phys. 119, 045902 (2016).